AD_____

Award Number: W81XWH-12-1-0442

TITLE: Targeting Estrogen-Induced COX-2 Activity in Lymphangioleiomyomatosis (LAM)

PRINCIPAL INVESTIGATOR: Jane Yu

CONTRACTING ORGANIZATION:

Brigham and Women's Hospital
Boston, MA 02115-0110

REPORT DATE: U&ƒ à^¦ 2013

TYPE OF REPORT: Annual Report

PREPARED FOR: U.S. Army Medical Research and Materiel Command
                       Fort Detrick, Maryland 21702-5012

DISTRIBUTION STATEMENT: Approved for Public Release; Distribution Unlimited

The views, opinions and/or findings contained in this report are those of the author(s) and should not be construed as an official Department of the Army position, policy or decision unless so designated by other documentation.

REPORT DOCUMENTATION PAGE

1. REPORT DATE	2. REPORT TYPE :	3. DATES COVERED:
October 2013	Annual	15September2012-14September2013

4. TITLE AND SUBTITLE

Targeting Estrogen-Induced COX-2 Activity in Lymphangioleiomyomatosis (LAM)

5a. CONTRACT NUMBER
W81XWH-12-1-0442

5b. GRANT NUMBER
W81XWH-12-1-0442

5c. PROGRAM ELEMENT NUMBER

6. AUTHOR(S)
Jane Yu

E-Mail: jyu13@rics.bwh.harvard.edu

5d. PROJECT NUMBER

5e. TASK NUMBER

5f. WORK UNIT NUMBER

7. PERFORMING ORGANIZATION NAME(S) AND ADDRESS(ES)

Brigham and Women's Hospital
One Blackfan Circle, Karp Bldg, 6th Fl,
Boston, MA 02115-5713

8. PERFORMING ORGANIZATION REPORT NUMBER

9. SPONSORING / MONITORING AGENCY NAME(S) AND ADDRESS(ES)
U.S. Army Medical Research and Materiel Command
Fort Detrick, Maryland 21702-5012

10. SPONSOR/MONITOR'S ACRONYM(S)

11. SPONSOR/MONITOR'S REPORT NUMBER(S)

12. DISTRIBUTION / AVAILABILITY STATEMENT

Approved for Public Release; Distribution Unlimited

13. SUPPLEMENTARY NOTES

Lymphangioleiomyomatosis (LAM), prostaglandin biosynthesis, cyclooxygenase-2 (COX-2), COX-2 inhibitors, xenografts rumors, bioluminescence, cell proliferation

14. ABSTRACT:

Lymphangioleiomyomatosis (LAM) is a progressive neoplastic disorder that leads to lung destruction and respiratory failure primarily in women. LAM is typically due to TSC2 mutations resulting in mTORC1 activation in proliferative smooth muscle-like cells in the lung. The female predominance of LAM suggests that estradiol contributes to disease development. Metabolomic profiling identified an estradiol-enhanced prostaglandin biosynthesis signature in Tsc2-deficient cells, both in vitro and in vivo. Estradiol increased the expression of cyclooxygenase-2 (COX-2), a rate-limiting enzyme in prostaglandin biosynthesis, which was also increased at baseline in TSC2-deficient cells, and was not affected by rapamycin treatment. However both Torin 1 treatment and Rictor knockdown, led to reduced COX-2 expression and phospho-Akt-S473. Prostaglandin production was also increased in TSC2-deficient cells. In preclinical models, both Celecoxib and aspirin reduced tumor development. LAM patients had significantly higher serum prostaglandin levels than healthy women. 15-epi-lipoxin-A4 was identified in exhaled breath condensate from LAM subjects and was increased by aspirin treatment, indicative of functional COX-2 expression in the LAM airway. In vitro, 15-epi-lipoxin-A4 reduced the proliferation of LAM patient-derived cells in a dose-dependent manner. Targeting COX-2 and prostaglandin pathways may have therapeutic value in LAM and TSC-related diseases, and possibly in other conditions associated with mTOR-hyperactivation.

15. SUBJECT TERMS none provided

16. SECURITY CLASSIFICATION OF:

a. REPORT	b. ABSTRACT	c. THIS PAGE	17. LIMITATION OF ABSTRACT	18. NUMBER OF PAGES	19a. NAME OF RESPONSIBLE PERSON USAMRMC
U	U	U	UU	5	19b. TELEPHONE NUMBER *(include area code)*

Table of Contents

INTRODUCTION:

This proposal is focused on the molecular mechanisms underlying the pathogenesis of lymphangioleiomyomatosis (LAM), a devastating pulmonary disease affecting exclusively young women, often leading to end-stage lung disease. LAM is believed to affect approximately 30% of women with tuberous sclerosis complex (TSC). The only proven treatment for LAM is lung transplantation, which carries significant one-year mortality and after which LAM can recur in the transplanted lungs. The pathogenesis of LAM is very unusual: LAM cells are histological benign smooth muscle cells carrying TSC1 or TSC2 mutations that are believed to metastasize to the lungs where they cause lung degeneration. Cells lacking TSC1 or TSC2 exhibit hyperactivation of the mammalian target of rapamycin complex 1 (TORC1), a master regulator of cell growth, protein translation, and metabolism. In LAM patients the TORC1 inhibitor Rapamycin stabilizes lung function and improves symptoms. Our central hypothesis is that E_2 induces COX-2 activity and production of prostaglandins (PGE2, PGD2, and 6-K-PGF1a), thereby promoting the survival and lung metastasis of TSC2-null cells. Furthermore, in preclinical models of LAM, molecular and pharmacologic suppression of COX-2 will block the E_2-promoted lung metastasis and induce a regression of established lung lesions.

BODY:
Aim 1. To examine the cellular impact of COX-2 in TSC2-null LAM patient-derived cells in vitro. We proposed to test whether COX-2 is a key mediator for E2-enhanced prostaglandin production. We have successfully established two independent clones of COX-2 shRNA in human lung epithelial cells (**Figure 1**). We will use the same set of shRNA-COX-2 to develop COX-2 knock-down LAM patient-derived cells. We have also developed the ELISA assay for measuring PGE2 and 6-K-PGF1a in conditioned media.

To inhibit COX-2 pharmacologically, we treated TSC2-deficient cells with aspirin or NS398, and found that both agents reduced COX-2 protein levels and production of PGE2 and 6-K-PGF1a. This result has been included in the manuscript (**Figure 4j-k**, Li et al., J Expt Med 2013, conditional acceptance, please see the **Appendix 1**). Moreover, aspirin or NS398 suppressed the proliferation of TSC2-deficient cells (**Figure 4l**, Li et al., J Expt Med 2013).

Aim 2. To determine whether the molecular depletion of COX-2 suppresses estrogen-promoted lung metastasis of LAM patient-derived cells in vivo. We have successfully established two independent clones of COX-2 shRNA in TSC2-null LAM patient-derived cells. We will perform the in vivo experiment in the second funding year. To measure COX-2 activity in tumors of TSC2-null cells, we used noninvasive live imaging-XenoLight RediJect COX-2 probe. However, we did not detect tumor specific COX-2 signals in mice bearing xenograft tumors. We will continue optimizing the reagent and monitor tumor COX-2 activity.

Aim 3. To determine whether the COX-2 inhibitor Celecoxib can reduce the burden of established tumors or block E_2-promoted lung metastases in preclinical models of LAM. We have treated mice with the COX-2 inhibitor aspirin, and measured xenograft tumor burden in a subcutaneous tumor model of TSC2-null cells. We found that aspirin treatment for three weeks decreased the intensity of bioluminescence (**Fig. 5c & d**), and decreased the tumor size (**Fig. 5e**). Tumors also had reduced expression of COX-2 and c-Myc, and increased levels of cleaved-caspase-3 and cleaved-PARP (**Fig. 5f**).

KEY RESEARCH ACCOMPLISHMENTS:
- COX-2 is a key mediator for E2-enhanced prostaglandin production
- Inhibition of COX-2 inhibits growth rate of TSC2-null cells
- Inhibition of COX-2 suppresses the growth of subcutaneous tumors

REPORTABLE OUTCOMES:
1. Oral presentation at The International LAMposium 2013. April, 2013, Cincinnati OH.
   "Aspirin inhibits cyclooxygenase 2-mediated prostaglandin production and tumorigenesis in a preclinical model of LAM." Yu, Jane et al.
2. Poster presentation at AACR-Frontier in Basic Cancer Research 2013. September, 2013, National Harbor, MD.
   "Tuberin negatively regulates the expression of cyclooxygenase 2 and prostaglandin production and tumorigenesis in a preclinical model of LAM." Yu, Jane et al.
3. Manuscript under final consideration-conditional accepted.

Chenggang Li*, Po-Shun Lee*, Yang Sun*, Xiaoxiao Gu, Erik Zhang, Yanan Guo, Chin-Lee Wu, Neil Auricchio, Carmen Priolo, Jing Li, Alfredo Csibi, Andery Parkhitko, Tasha Morrison, Anna Planaguma, Shamsah Kazani, Elliot Israel, Kai-Feng Xu, Elizabeth Petri Henske, John Blenis, Bruce D Levy, David Kwiatkowski and **Jane J. Yu**. Estradiol and mTORC2 orchestrate to enhance prostaglandin biosynthesis and tumorigenesis in tuberous sclerosis complex. **J Expt Med 2013.**

CONCLUSION:

LAM is often a progressive disease which leads to respiratory failure and death in the absence of lung transplantation. The recent demonstration that rapamycin has clinical benefit in LAM is a major success. However, not all patients respond to rapamycin, and upon rapamycin withdrawal, lung function decline resumes. Hence lifelong treatment of LAM patients with rapamycin may be required to maintain benefit, with unknown long-term toxicities. Our findings suggest that aspirin and/or other COX-1/COX-2 inhibitors may have significant benefit in slowing LAM progression. The well-known side-effect and toxicity profile of these drugs make them attractive candidates for long-term therapy in LAM patients. It is also possible that other neoplastic conditions associated with mTOR hyperactivation could be responsive to these agents. Further preclinical and clinical investigation is warranted to explore these possibilities.

REFERENCES:

Chenggang Li*, Po-Shun Lee*, Yang Sun*, Xiaoxiao Gu, Erik Zhang, Yanan Guo, Chin-Lee Wu, Neil Auricchio, Carmen Priolo, Jing Li, Alfredo Csibi, Andery Parkhitko, Tasha Morrison, Anna Planaguma, Shamsah Kazani, Elliot Israel, Kai-Feng Xu, Elizabeth Petri Henske, John Blenis, Bruce D Levy, David Kwiatkowski and **Jane J. Yu**. Estradiol and mTORC2 orchestrate to enhance prostaglandin biosynthesis and tumorigenesis in tuberous sclerosis complex. **J Expt Med 2013. (**Under final consideration**)**

APPENDICES:

Manuscript under final consideration-conditional accepted. (pdf file is attached)
Chenggang Li*, Po-Shun Lee*, Yang Sun*, Xiaoxiao Gu, Erik Zhang, Yanan Guo, Chin-Lee Wu, Neil Auricchio, Carmen Priolo, Jing Li, Alfredo Csibi, Andery Parkhitko, Tasha Morrison, Anna Planaguma, Shamsah Kazani, Elliot Israel, Kai-Feng Xu, Elizabeth Petri Henske, John Blenis, Bruce D Levy, David Kwiatkowski and **Jane J. Yu**. Estradiol and mTORC2 orchestrate to enhance prostaglandin biosynthesis and tumorigenesis in tuberous sclerosis complex. **J Expt Med 2013.**
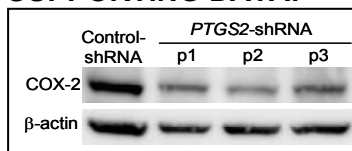
SUPPORTING DATA:

Figure 1. **Development of stable cells in which COX-2 is depleted.** Human bronchial epithelial BEAS-2A cells were infected with lentiviral shRNA against *PTGS2* (COX-2) and grown with puromycin 3 µg/ml for 1 week. After selection the cells were grown with puromycin 1 µg/ml. COX-2 levels were examined at passages p1-p3.

Estradiol and mTORC2 orchestrate to enhance prostaglandin biosynthesis and tumorigenesis in tuberous sclerosis complex

Chenggang Li[1*], Po-Shun Lee[1*], Yang Sun[1*], Xiaoxiao Gu[2], Erik Zhang[1], Yanan Guo[1], Chin-Lee Wu[3], Neil Auricchio[1], Carmen Priolo[1], Jing Li[2], Alfredo Csibi[2], Andrey Parkhitko[1], Tasha Morrison[1], Anna Planaguma[4], Shamsah Kazani[4], Elliot Israel[4], Kai-Feng Xu[5], Elizabeth Petri Henske[1], John Blenis[2], Bruce D. Levy[4], David Kwiatkowski[1†], and Jane Yu[1†]

[1]Brigham and Women's Hospital/Harvard Medical School, One Blackfan Circle, 6th Floor, Boston, MA 02115; [2]Harvard Medical School, Boston, MA; [3]Massachusette General Hospital, Boston, MA; [4]Pulmonary and Critical Care Medicine, Department of Internal Medicine, Brigham and Women's Hospital and Harvard Medical School, Boston, MA; [5]Peking Union Medical College, Beijing, China

*Equal contribution †Co-correspondence

Running title: Tuberin inhibits COX-2 in TSC

Key words: TSC2; estradiol; prostaglandin metabolism; aspirin; mTORC2; cyclooxygenases

Address correspondence to:
Jane Yu, Brigham and Women's Hospital/Harvard Medical School, One Blackfan Circle, 6th Floor, Boston, MA 02115
Tel: 617 355 9018; Fax: 617 355-9016; E-mail: jyu13@partners.org
(Designated author for communication)

and

David Kwiatkowski, Brigham and Women's Hospital/Harvard Medical School, One Blackfan Circle, Boston, MA 02115
Tel: 617-355-9005; Fax: 617-355-9016; Email: dkwiatkowski@rics.bwh.harvard.edu

Number of Characters (with space): 35,415

Abstract

Lymphangioleiomyomatosis (LAM) is a progressive neoplastic disorder that leads to lung destruction and respiratory failure primarily in women. LAM is typically due to TSC2 mutations resulting in mTORC1 activation in proliferative smooth muscle-like cells in the lung. The female predominance of LAM suggests that estradiol contributes to disease development. Metabolomic profiling identified an estradiol-enhanced prostaglandin biosynthesis signature in Tsc2-deficient cells, both *in vitro* and *in vivo*. Estradiol increased the expression of cyclooxygenase-2 (COX-2), a rate-limiting enzyme in prostaglandin biosynthesis, which was also increased at baseline in TSC2-deficient cells, and was not affected by rapamycin treatment. However both Torin 1 treatment and Rictor knockdown, led to reduced COX-2 expression and phospho-Akt-S473. Prostaglandin production was also increased in TSC2-deficient cells. In preclinical models, both Celecoxib and aspirin reduced tumor development. LAM patients had significantly higher serum prostaglandin levels than healthy women. 15-epi-lipoxin-A_4 was identified in exhaled breath condensate from LAM subjects and was increased by aspirin treatment, indicative of functional COX-2 expression in the LAM airway. *In vitro*, 15-epi-lipoxin-A_4 reduced the proliferation of LAM patient-derived cells in a dose-dependent manner. Targeting COX-2 and prostaglandin pathways may have therapeutic value in LAM and TSC-related diseases, and possibly in other conditions associated with mTOR-hyperactivation.

Introduction

Lymphangioleiomyomatosis (LAM) is a progressive pulmonary disease which affects almost exclusively women. LAM is characterized pathologically by widespread proliferation of abnormal smooth muscle cells that typically have Tuberous Sclerosis Complex (*TSC) 2* mutation leading to mTORC1-activation, and by cystic changes within the lung parenchyma (Henske and McCormack; Krymskaya; McCormack et al., 2010; McCormack et al.; Taveira-Dasilva et al.). LAM occurs in 30-40% of women with tuberous sclerosis complex (TSC) (Costello et al., 2000; Dabora et al., 2001). However, LAM is more commonly diagnosed in women who do not have clinical features of TSC or germline mutations in *TSC1* or *TSC2* ("sporadic LAM"). Inactivating mutations of both alleles of the *TSC1* or *TSC2* genes have been found in LAM cells from both TSC-LAM and sporadic LAM patients (Astrinidis et al., 2000; Strizheva et al., 2001).

About 60% of women with the sporadic form of LAM also have renal angiomyolipomas (Ryu et al., 2012). The presence of *TSC2* mutations in LAM cells and renal angiomyolipoma cells from women with sporadic LAM, but not in normal tissues, has led to the model that LAM cells spread to the lungs via a metastatic mechanism, despite the fact that LAM cells have a histologically benign appearance (Astrinidis et al., 2000; Karbowniczek et al., 2003) (Crino et al., 2006). Genetic and molecular analyses of recurrent LAM after lung transplantation support this benign metastatic model (Karbowniczek et al., 2003).

The protein products of *TSC1* and *TSC2*, hamartin and tuberin, respectively, form a heterodimer (Jaeschke et al., 2002; Plank et al., 1998) that inhibits the small GTPase Rheb (Ras homologue

enriched in brain), via tuberin's highly conserved GTPase activating protein (GAP) domain. Loss of tuberin or hamartin leads to hyperactivation of the mammalian target of Rapamycin complex 1 (mTORC1), in both LAM cells, other TSC tumors, and multiple animal models (Manning, 2010). mTORC1 regulates cell growth, protein translation and metabolism (Duvel et al.). In a randomized MILES trial (Multicenter International LAM Efficacy of Sirolimus Trial), the mTORC1 inhibitor rapamycin stabilized lung function and improved symptoms in LAM patients (McCormack et al., 2011). However, lung function declined when rapamycin was discontinued.

The female predominance of LAM strongly suggests that estradiol contributes to disease pathogenesis (Henske and McCormack; McCormack et al.). We have demonstrated that estradiol treatment increases levels of circulating tumor cells and pulmonary metastases of TSC2-deficient cells in a xenograft model of LAM (Yu et al., 2009). Other studies have demonstrated that estradiol induces COX-2-mediated prostaglandin synthesis (Egan et al., 2004). COX-2 is a rate-limiting enzyme catalyzing the conversion of arachidonate to prostaglandins. COX-2 overexpression has been documented in human tumors, and prostaglandins may contribute to cancer development (FitzGerald and Patrono, 2001; Muller, 2004; Wang and Dubois; Wang et al., 2007). In this study, we discovered that estradiol enhances prostaglandin production by TSC2-deficient cells. Furthermore, loss of TSC2 increases COX-2 and prostaglandin biosynthesis in a rapamycin-insensitive but Torin 1-sensitive and Rictor-dependent manner, suggesting an mTORC1-independent but mTORC2-dependent mechanism. We also showed that loss of TSC2 leads to alterations in the cellular distribution of EGFR, and this appears to be the mechanism by which it causes increased PG biosynthesis. Celecoxib reduced

renal tumor incidence in a spontaneous-arising $Tsc2^{+/-}$ mouse tumor model, and aspirin suppressed tumor progression in a xenograft tumor model. This study indicates that targeting COX-2 with aspirin or related drugs may have therapeutic benefit in LAM and TSC-related diseases.

Results

Identification of an estradiol-induced prostaglandin biosynthesis signature in TSC2-deficient cells *in vitro* and *in vivo*

To examine the possible effects of estradiol on metabolic pathways in Tsc2-deficient rat-uterus-derived ELT3 cells, we performed a metabolomic screen. A significant increase in prostaglandins including PGE_2, PGD_2, and 6-keto-$PGF_{1\alpha}$, was seen in estradiol-treated cells (**Fig. 1a**). Furthermore, estradiol increased p44/42-MAPK T202/Y204 phosphorylation, COX-2 expression, and PGE_2 levels in Tsc2-deficient cells at 2 and 24 hr (**Fig. 1b, c**). Analysis of LAM patient-derived TSC2-deficient 621-101 cells (Yu et al., 2004) showed that estradiol also increased PGE_2 levels at 24 hr (**Fig. 1d**), confirming the results in the Tsc2-deficient ELT3 cells.

To define the impact of estradiol on activation of signaling pathways, we first compared the basal levels of phospho-S6, phospho-MAPK and phospho-Akt S473 for the TSC2+/+ and TSC2-/- cells. TSC2-deficient cells (TSC2-) exhibited lower level of phospho-Akt S473, higher levels of phospho-MAPK and phospho-S6, relative to TSC2-reexpressing cells (TSC2+) (**Fig. 1e**). We next performed a time course analysis of the effect of estradiol on activation of these pathways in both TSC2-deficient (TSC-) and TSC2-reexpressing (TSC2+) LAM-derived cells. We found that estradiol activated Akt S473 within 6 hr, MAPK (T202Y204) at 2, 4, 6, 8 & 24 hr, but not S6 in

TSC2- cells (**Fig.1f**, left panel). In comparison, estradiol stimulated Akt S473 and MAPK (T202Y204) to much lesser degree in TSC2-reexpressing (TSC2+) cells (**Fig. 1f**, right panel). Our data indicate that estradiol activates MAPK and Akt pathways in the absence of TSC2.

To determine whether the effect of estradiol on TSC2-deficient cells is dependent on TSC defects, we examined the levels of COX-2 using immunoblotting in estradiol-stimulated TSC2-deficient and TSC2-reexpressing cells. Estradiol treatment did not affect COX-2 expression in TSC2-reexpressing LAM patient-derived cells (**Fig. 1g**). To address how estradiol exerts its action on COX-2 expression and prostaglandin production, we examined the activation of p44/42-MAPK and PI3K/Akt, which are known pathways promoting COX-2 expression (Wang and Dubois, 2010). We found that estrogen activates both p44/42-MAPK and PI3K/Akt in TSC2-deficient cells, assessed by phosphorylation at T202/204 and S473 sites respectively, but not in TSC2-reexpressing cells (**Fig. 1g, h**). Inhibition of p44/42-MAPK using PD98059 or PI3K/Akt using PI-103 blocked estrogen-enhanced COX-2 expression (**Fig. 1i, j**). Collectively, these data indicate that estradiol activates COX-2 expression via p44/42-MAPK and PI3K/Akt pathways.

To determine the effect of estradiol on cellular metabolism *in vivo*, we used xenograft tumors of Tsc2-deficient ELT3 cells (Yu et al., 2009) from placebo or estradiol-implanted ovariectomized female mice, in which p44/42-MAPK phosphorylation was evident (**Fig. 1k**). A metabolomic screen showed that levels of PGE_2, PGD_2, 6-keto-$PGF_{1\alpha}$ was significantly increased in xenograft tumors from mice treated with estradiol (**Fig. 1l**), Estradiol-treated mice bearing ELT3 xenograft tumors also exhibited higher levels of urinary PGE_2 relative to placebo controls (**Fig. 1m**). These

data demonstrate that estradiol stimulates prostaglandin biosynthesis by TSC2-deficient cells *in vitro* and *in vivo*.

TSC2 negatively regulates COX-2 expression and prostaglandin production *in vitro* and *in vivo*.

Prostaglandins are products of prostaglandin-endoperoxide synthases (PTGS) 1 and 2, or more commonly known as COX-1 and COX-2 (**Fig. 2**). COX-1 and COX-2 convert arachidonic acids released from membrane phospholipids into PGH_2. Prostacyclin (PGI_2) is produced by prostacyclin synthase (PTGIS) from PGH_2 (**Fig. 2a**). To define the molecular mechanisms responsible for estradiol-enhanced COX-2 expression and prostaglandin production, we analyzed our previous expression array of TSC2-deficient LAM patient-derived cells (Lee et al., 2010) and found that both COX-2 (*PTGS2*) and prostacyclin synthase (*PGTIS)* expression were significantly increased, by 2-fold and 40-fold respectively (**Fig. 2b and Table 1**), in TSC2-deficient cells relative to TSC2-reexpressing cells. To validate the findings of the expression array, we first performed real-time RT-PCR analysis. TSC2-deficient LAM patient-derived cells exhibited 102-fold increase of PTGS2, and 15-fold increase of PTGIS ($p < 0.0001$, **Fig. 2c**). Importantly, rapamycin treatment did not affect the levels of PTGS2, but increased the levels of PTGIS by 6.6-fold ($p < 0.05$, **Fig. 2c**), consistent with the changes identified in the expression array profile (Lee et al., 2010) (Fig. 2b). We next examined the protein levels of COX-2 and PTGIS using immunoblotting analysis. COX-2 protein levels were higher in TSC2-deficient cells compared to TSC2 reexpressing 621-101 cells (**Fig. 2d**). Rapamycin treatment suppressed phosphorylation of the ribosomal protein p70S6 (S6), but did not affect the level of COX-2 expression, although it altered the migration of COX-2 (**Fig. 2d**). COX-2 occurs as 72 and 74kDa isoforms, with the

larger form due to glycosylation at Asn580 (Sevigny et al., 2006). LAM cells treated with tunicamycin, an inhibitor of N-acetylglucosamine transferases, showed a marked reduction in the slower migrating form of COX-2, but showed similar production of PGE_2 (**Fig. 2e**). This implies that this gel-shift of COX-2 is due to increased glycosylation.

Prostacyclin synthase (PTGIS) catalyzes the conversion of PGH_2 to prostacyclin (PGI_2). PTGIS protein levels were markedly higher in TSC2-deficient cells compared to TSC2 reexpressing 621-101 cells (**Fig. 2f**). Rapamycin treatment suppressed phosphorylation of the ribosomal protein p70S6 (S6), and decreased PTGIS levels in TSC2-deficient cells to a minor extent, but had no appreciable effect on TSC2-reexpressing cells (**Fig. 2f**), suggesting that TSC2 also regulates PTGIS expression independent of mTORC1.

To determine the functional impact of altered expression COX-2 and PGTIS on prostaglandin production, secreted levels of PGEM (a stable PGE_2 metabolite), 6-keto-$PGF_{1\alpha}$ (a stable prostacyclin PGI_2 metabolite), and $PGF_{2\alpha}$ were measured from TSC2-deficient LAM patient-derived cells treated with rapamycin or control. Levels of PGE_2, 6-keto-$PGF_{1\alpha}$, and $PGF_{2\alpha}$ were all significantly higher in TSC2-deficient cells relative to TSC2-reexpressing cells, and were also insensitive to rapamycin treatment (**Fig. 2g**). Similar results on COX-2 expression were also seen in Tsc2-deficient ELT3 cells (**Fig. 2h**). PGE_2 levels were elevated by 2.5-fold in ELT3 cells in comparison to TSC2 reexpressing cells, and this again was not affected by rapamycin treatment (**Fig. 2i**). To determine whether this phenomenon of rapamycin-insensitive prostaglandin production was seen in other cancer cells with intact TSC2 levels but mTORC1 activation, we examined HeLa, U2OS and OVCAR5 cells. Although PGE_2 production was variable among

these cell lines, rapamycin did not affect COX-2 expression or PGE_2 production though reducing phospho-S6 (**Fig. 2j & k**). Together, these data indicate that upregulation of COX-2 and prostaglandin production is rapamycin-insensitive in cells with mTORC1 activation.

To determine whether TSC2 regulates COX-2 and prostaglandin production *in vivo*, we used xenograft tumors from mice inoculated with Tsc2-deficient ELT3-V3 (vector-control) cells and TSC2-addback ELT3-T3 cells. COX-2 levels were significantly higher in the ELT3-V3 xenograft tumors with elevated phospho-S6 relative to TSC2-addback ELT3-T3 tumors (**Fig. 3a**). In addition, levels of PGE_2 in xenograft tumors were significantly higher in mice with the ELT3-V3 tumors in comparison to mice with the TSC2-addback ELT3-T3 tumors (**Fig. 3b**). Moreover, urinary PGE_2 level was significantly higher in mice with the ELT3-V3 tumors in comparison to mice with the TSC2-addback ELT3-T3 tumors (**Fig. 3c**). Similar results on PGTIS expression were also observed in xenograft tumors of Tsc2-deficient ELT3 cells (**Fig. 3d**). Urinary 6-keto-PGF1α levels were also significantly higher in mice with the ELT3-V3 tumors in comparison to mice with the TSC2-addback ELT3-T3 tumors (**Fig. 3e**). Together, these data indicate that upregulation of COX-2 and prostaglandin production is rapamycin-insensitive in cells with mTORC1 activation

mTORC2 is a critical mediator of COX-2 expression and prostaglandin biosynthesis in TSC2-deficient cells.

To identify additional molecular determinants responsible for rapamycin-insensitive COX-2 expression and prostaglandin biosynthesis, we first treated $Tsc2^{-/-}p53^{-/-}$ MEFs with Torin 1, a potent ATP-competitive mTORC1 and mTORC2 inhibitor for 24 hr. Torin 1 decreased the level

of COX-2 and phosphorylation of S6 (S235/236) and 4EBP1. Interestingly, cells treated with LY294002, a PI3K inhibitor, for 24 hr, exhibited reduced level of COX-2. However, rapamycin treatment did not affect the level of COX-2 (**Fig. 4a**). Our data suggest that mTORC2 might play a role in mediating COX-2 expression. To further test the impact of mTORC2 on COX-2 expression, we generated stable knockdown of Rictor, an mTORC2 component, in $Tsc2^{-/-}p53^{-/-}$ MEFs. Rictor silencing profoundly decreased the level of COX-2 and phosphorylation of S6, supporting the notion that mTORC2 is a critical mediator of COX-2 expression in TSC2-deficient cells (**Fig. 4b**). Moreover, we found that Rictor knockdown markedly reduced phosphorylation of Akt (S473), a direct target of mTORC2 (**Fig. 4c**), indicating the potential impact of mTORC2-Akt axis on COX-2 expression in $Tsc2^{-/-}p53^{-/-}$ MEFs. Why does 4a look so different from 4d – note that COX-2 is reduced a little with Torin1 in 4a, while it's gone in 4d?

To examine the effect of Torin 1 on COX-2 expression in LAM patient-derived cells, we treated 621-101 cells with Torin 1 for 24 hr. Torin 1 markedly decreased the level of COX-2. However, rapamycin treatment did not affect COX-2 expression in TSC2-deficient 621-101 cells. NS398, a COX-2 inhibitor, strongly decreased the levels of COX-2 in TSC2-deficient cells (**Fig. 4d**). Interestingly, Torin 1 treatment decreased phosphorylation of both p44/42-MAPK T202/Y204 and PI3K/Akt S473 (**Fig. 4e**). To prove that Akt is a critical mediator of COX-2 expression in LAM patient-derived cells, we treated 621-101 cells with PI-103 (a dual inhibitor of PI3K and mTOR), or Akt-VIII (a selective Akt inhibitor), for 24 hr, and found that both inhibitors strongly decreased the levels of COX-2 without affecting COX-1 (**Fig. 4f**).

It has been reported that TSC2 does not regulate mTORC2 activation (Dalle Pezze et al., 2012). We have found that mTORC2 is involved in COX-2 expression in TSC2-deficient cells. In another experiments, we found that COX-2 expression was decreased partially by treatment of PD98059 (MEK1/2 inhibitor) or PI-103 (Akt inhibitor), but more strongly by the combination of PD98059 and PI-103 (**Fig. 4g**), suggesting that both MEK1/2-MAPK and PI3K/Akt pathways contribute to COX-2 expression. Collectively, our data indicate that mTORC2-Akt plays a critical role in mediating COX-2 expression in TSC2-deficient cells.

To further define the mechanism by which TSC2 acts as a negative regulator of COX-2 protein expression, we focused on epidermal growth factor receptor (EGFR), a known regulator of COX-2 expression and prostaglandin production (Brand et al., 2013; Mann et al., 2005). We found that TSC2-deficient cells treated with anti-EGFR agents, Afatinib and Gefitinib, exhibited decreased levels of COX-2 protein, compared to vehicle control (**Fig. 4h**). Interestingly, using confocal microscopy, we observed that TSC2 deficiency resulted in abundant nuclear localization of EGFR in comparison with TSC2-reexpression in two cell types, rat uterine leiomyoma-derived and LAM patient-derived cells (**Fig. 4i**). Furthermore, EGFR nuclear localization was not affected by rapamycin treatment (**Fig. 4i**), supporting rapamycin-insensitive upregulation of COX-2 expression and prostaglandin production. Concomitantly, two PI3K/Akt inhibitors Akt VIII or PI-103 treatment suppressed COX-2 expression (Fig. 4f, g). Together, these data support a model in which TSC2 negatively regulates COX-2 expression via effects on nuclear and cytoplasmic localization of EGFR.

Aspirin treatment inhibits the proliferation of TSC2-deficient cell and reduces urinary levels of prostaglandins *in vitro*.

To determine whether inhibition COX-2 impacts the proliferation of TSC2-deficient cells, we treated 621-101 cells with Sulindac (a COX-1 inhibitor), NS398 (a COX-2 inhibitor), or aspirin (an irreversible COX-1 and COX-2 inhibitor by blocking their enzymatic activities, and also acetylates COX-2, resulting in production of 15-epi-LXA$_4$, an anti-inflammatory/antitumor compound) for 24 hr. NS398 and aspirin reduced COX-2 and COX-1 levels without affecting phosphorylation of p44/42-MAPK or S6 (**Fig. 4j**). Aspirin significantly decreased PGE$_2$ levels (**Fig. 4k**), and reduced proliferation of 621-101 cells (**Fig. 4l**).

Inhibition of COX-2 suppresses renal tumorigenesis and inhibits the progression of xenograft tumor of Tsc2-deficient cells in preclinical models.

To determine the efficacy of inhibition of COX-2 *in vivo*, first, we used the COX-2 specific inhibitor Celecoxib to treat *Tsc2*$^{+/-}$ mice, which develop spontaneous renal cystadenomas at age of 4 months. We found that treatment with Celecoxib strongly suppressed microscopic renal lesions in *Tsc2*$^{+/-}$ mice by ~50% following four month of treatment (0.1% w/w in chow) relative to vehicle control (**Fig. 5a & b**). These data indicate that COX-2 is responsible for renal tumorigenesis.

We next assessed the possible benefit of aspirin in a xenograft tumor model of Tsc2-deficient ELT3-luciferase-expressing cells. Aspirin treatment for three weeks decreased the intensity of bioluminescence (**Fig. 5c & d**), and decreased the tumor size (**Fig. 5e**). Tumors also had reduced expression of COX-2 and c-Myc, and increased levels of cleaved-caspase-3 and cleaved-PARP

(**Fig. 5f**). Aspirin-treated mice bearing ELT3 xenograft tumors had markedly reduced urinary levels of PGE_2 (**Fig. 5g**), consistent with strong inhibition of each of COX-1 and COX-2, as expected (**Fig. 4j**). These data indicate that aspirin reduces PGE_2 production and tumor growth in this Tsc2-deficient xenograft model.

Evidence for COX-2 activation *in vivo* in LAM

We then examined whether these *in vitro* and xenograft model findings were relevant to human LAM. Accordingly, LAM lungs were found to express higher levels of COX-2 (PTGS2) in comparison to control lungs (**Fig. 6a**). Furthermore, immunohistochemistry analyses showed that COX-2 expression was specifically increased in pulmonary LAM nodules (arrows), which were also expressed both smooth muscle actin (SMA) and phospho-S6 (**Fig. 6b**). To examine the functional effects of COX-2 expression in LAM, 15-epi-lipoxin A_4 (LXA_4), a product of aspirin-acetylated COX-2, was measured in exhaled breath condensate (EBC) from three LAM subjects (**Table 2**). LXA_4 was detected in EBC and the levels were increased with aspirin (**Fig. 6c**). Of interest, LXA_4 decreases proliferation of A549 cells (Human lung adenocarcinoma) (Claria et al., 1996) and also reduced the growth of LAM patient-derived 621-101 cells at 100 nM (**Fig. 6d**). In a separate experiment, the 15-epi-LXA4 integrity was confirmed by UV-Vis spectrophotometry to ensure the presence of the diagnostic tetraene chromophore and accurate quantitation and HPLC to ensure that only a single peak was present without evidence for isomerization. (**Fig. 6e**). We next performed a dose-response of LXA_4 and found that LXA_4 at 500 nM exhibited the strongest inhibitory effect on cell growth (**Fig. 6e**).

Urinary PGE_2 levels were measured in 29 LAM patients and in 18 healthy women; however, these levels were not significantly different between two groups (**Fig. 6f**). Because renal prostaglandin production can significantly influence urinary prostaglandin levels, we next measured PGE_2 and 6-keto-$PGF_{1\alpha}$ levels in sera from 14 LAM patients and 13 healthy women. Of note, the mean serum PGE_2 level of LAM patients (27.8 ± 1.8 pg/mL) was higher than that of healthy women (19.6 ± 1.4 pg/mL, $p = 0.0021$) (**Fig. 6g**). In addition, the mean serum 6-keto-PGF1α level of LAM patients (192.2 ± 64.9 pg/mL) was also higher compared with the mean in healthy women (82.6 ± 6.3 pg/mL, $p = 0.0006$) (**Fig. 6h**).

Discussion

LAM is a neoplastic disorder in which smooth muscle-like cells with biallelic inactivation of *TSC2* leads to hyperactivation of mTORC1. This fundamental mechanistic insight led to the recent reported success in treating LAM patients with rapamycin. However, mTORC1 independent effects of TSC2-loss are also known (Neuman and Henske; Yu and Henske, 2010). The marked female predominance of LAM suggests that estradiol promotes disease progression. In this study, we identified an estradiol-induced prostaglandin metabolic signature in Tsc2-deficient ELT3 cells *in vitro* and *in vivo*. Prostaglandins, synthesized via COX-1/COX-2, appear to play important roles in cancer progression (FitzGerald and Patrono, 2001; Muller, 2004; Wang and Dubois; Wang et al., 2007), although their precise role is still hotly debated. Estradiol-dependent prostaglandin production has been studied in other models. Estradiol activated COX-2 and increased prostacyclin synthesis in mouse aortic smooth muscle cells (Egan et al., 2004). Increased levels of PGE_2 causes enhanced aromatase expression and local estradiol production in breast tissue (Subbaramaiah et al.). However, the relationship between prostaglandins and

TSC/LAM has not been investigated previously. Remarkably, we found that estradiol enhances the expression of COX-2 and induces production of PGE_2 in TSC2-deficient cells *in vitro* and *in vivo*. Furthermore, we identified a novel function of TSC2 as a negative regulator of COX-2 expression and prostaglandin biosynthesis. Interestingly, this regulation appears to be rapamycin-insensitive but sensitive to Akt inhibition and rictor knockdown, suggesting that COX-2 may be regulated by Akt in TSC2-deficient cells.

We also demonstrated that COX-2 is abundant in LAM lesions, and that serum levels of PGE_2 are elevated in LAM patients. Collectively, our data suggest that COX-2 may play an important role in LAM pathogenesis.

NS398 and aspirin are direct enzyme inhibitors of COX-2 and/or COX-1. As expected, we have found that cells treated with NS398 or aspirin exhibited reduced levels of PGE_2 (Fig. 4k), consistent with this inhibition. However, we also found that both NS398 and aspirin decreased the levels of COX-2 protein. Although this was initially surprising to us, multiple experiments confirmed this effect, and our results are in agreement with previous reports that COX-2 protein expression is reduced by classical NSAIDs including aspirin and NS398 (Galamb et al., 2010; Takada et al., 2004). Therefore, we think that both enzymatic inhibition and reduction in expression of COX-2 occurs in response to NS398 and aspirin treatment. Aspirin, the prototypical non-steroidal anti-inflammatory drug, covalently modifies both COX-1 and COX-2 by acetylation. We demonstrated that aspirin treatment significantly reduced the growth of xenograft tumors of Tsc2-deficient ELT3 cells, and led to reduced urinary levels of PGE_2 and 6-keto-PGF1α consistent with strong inhibition of COX-1/COX-2 function. Furthermore, xenograft

tumors from aspirin-treated mice exhibited higher levels of apoptosis compared to vehicle-treatment (Fig. 5f). While aspirin-acetylated COX-2 inhibits prostaglandin formation, the enzyme is not completely inactivated. Rather, aspirin-acetylated COX-2 catalyzes the conversion of arachidonate to 15-epi-LXA$_4$ (Claria et al., 1996). In this manner, aspirin both inhibits prostaglandin production and triggers the formation of 15-epi-LXA$_4$, a potent inhibitor of malignant cell proliferation (Claria et al., 1996). 15-epi-LXA$_4$ was present in EBC from LAM patients, and was increased with oral aspirin ingestion. 15-epi-LXA$_4$ also decreased LAM-patient-derived cell proliferation (**Fig. 6d**, **e**) Together, these findings suggest that aspirin may have rapamycin-independent beneficial effects in LAM.

LAM is often a progressive disease which leads to respiratory failure and death in the absence of lung transplantation. The recent demonstration that rapamycin has clinical benefit in LAM is a major success. However, not all patients respond to rapamycin, and upon rapamycin withdrawal, lung function decline resumes (McCormack et al.). Hence lifelong treatment of LAM patients with rapamycin may be required to maintain benefit, with unknown long-term toxicities. Our findings suggest that aspirin and/or other COX-1/COX-2 inhibitors may have significant benefit in slowing LAM progression. The well-known side-effect and toxicity profile of these drugs make them attractive candidates for long-term therapy in LAM patients. It is also possible that other neoplastic conditions associated with mTOR hyperactivation could be responsive to these agents. Further preclinical and clinical investigation is warranted to explore these possibilities.

Materials and Methods

Cell culture and reagents. ELT3 cells (Eker rat uterine leiomyoma-derived) (Howe et al., 1995a; Howe et al., 1995b) and LAM patient-derived 621-101, 621-102, and 621-103 cells were cultured in IIA complete medium. $Tsc2^{-/-}p53^{-/-}$ MEFs, HEK293, HeLa, U2OS and OVARC5 cells were cultured in DMEM supplemented with 10% FBS. 17-beta-estradiol (10 nM, Sigma), rapamycin (20 nM, Biomols), Torin 1 (250 nM, Tocris), LY294002 (20 µM, Cell Signaling), NS398 (50 µM, Cayman), Sulindac (50 µM, Cayman), aspirin (450 µM, Sigma), Celecoxib (Novartis), PI-103 (5 µM, Tocris), and AktVIII (5 µM, from Calbiochem), Wortmannin (1 µM, Cell Signaling) were used as indicated. 15-epi-LXA$_4$ (10 - 500 nM) is a Calbiochem product (Catalog #437725) and distributed by Millipore. The integrity of 15-epi-LXA$_4$ was determined by UV-Vis spectrometry and HPLC. Because of the volatile nature of this product, stock solutions were stored at -80°C.

Animal studies. All animal work was performed in accordance with protocols approved by the IACUC-CHB. For xenograft tumor establishment, 2 x 10^6 ELT3-luciferase cells were inoculated bilaterally into the posterior back region of female intact CB17-SCID mice (Taconic) as previously described (Liu et al.; Parkhitko et al.; Yu et al., 2009). Five-weeks post cell inoculation, mice bearing subcutaneous tumors were randomized into two groups: Vehicle control (n = 5), and aspirin (n = 5; 100 mg/kg/day, in drinking water). Tumor area (width x length) was measured weekly using a Calipers. Urine specimens were collected from mice for PGE$_2$ and 6-keto-PGF1$_\alpha$ measurement. For spontaneously-arising renal tumor model, $Tsc2^{+/-}$ mice, originally generated in this laboratory (Onda et al., 1999), were serially crossed with A/J mice for over five generations. These pure strain mice were used in all experiments. Celecoxib (Novartis) was administered by mouse chow (0.1%) for four months, beginning age one month, and then sacrificed for renal tumor assessment at the end of treatment, age five months.

Microscopic kidney tumor scores. Mouse kidneys were removed rapidly after euthanasia, and fixed overnight in 10% formalin. Kidneys were then prepared for histologic evaluation in stereotypical fashion by cutting the kidney into sections at 1 mm intervals throughout its length. Microscopic kidney tumor scores were determined in a semi-quantitative fashion by a single blinded observer. The set of 1 mm interval sections were prepared as H&E-stained 8 micrometer sections. Each tumor or cyst identified was measured to determine its length and width in two dimensions, as well as the percent of the lumen filled by tumor (this was 0% for a simple cyst, and 100% for a completely filled, solid adenoma). These measurements were converted into a measurement of tumor volume per lesion using the following formula. Tumor volume = maximum (tumor percent, 5)/100 * 3.14159/6 * 1.64 * (tumor length * tumor width)**1.5 (Auricchio et al.). The total tumor volume per kidney was then equal to sum of the tumor volume of each lesion identified. Comparisons between sets of mice for tumor measurements were made using the non-parametric Mann Whitney test in Prism (GraphPad Software, Inc., v4.0a).

Bioluminescent reporter imaging. Ten minutes prior to imaging, animals were injected with luciferin (Xenogen) (120 mg/kg, i.p.). Bioluminescent signals were recorded using the Xenogen IVIS System. Total photon flux of tumors was analyzed as previously described (Yu et al., 2009).

Confocal Microscopy. ELT3 cells and LAM-derived cells were plated on glass coverslips in 12-well tissue culture plates for overnight. Cells were serum starved overnight, and then treated with 20 nM rapamycin for 24 hr. Cells were rinsed with PBS twice, fixed with warm 4% paraformaldehyde, permeabilized with 0.2% Triton X-100, blocked in 3% BSA/PBS for 1 hr, and then incubated with primary antibody 1% BSA in PBS for 1 hr at room temperature

17

secondary antibodies for 1 hr. Images were captured with a FluoView FV-10i Olympus Laser Point Scanning Confocal Microscope.

Expression array analysis. Re-analysis of previously published expression array data (GEO accession number GSE16944) (Lee et al, 2009) was performed using an online tool GEO2R. Transcript levels of *PTGS2* (COX-2) (ID: 238018) and *PTGIS* (prostacyclin synthase) (ID: 454010) were compared between TSC2-deficient (TSC2-) and TSC2-addback (TSC2+) cells, or rapamycin-treated and vehicle-treated TSC2-deficient (TSC2-).

Quantitative RT-PCR. RNA from cultured cells and xenograft tumors was isolated using RNeasy Mini Kit (Qiagen). Gene expression was quantified using One-Step qRT-PCR Kits (Invitrogen) in the Applied Biosystems Step One Plus Real-Time PCR System and normalized to beta-actin.

Immunoblotting and antibodies. Cells were lysed in m-PER buffer (Pierce). Antibodies were used: COX-1, COX-2, EGFR, phospho-p44/42-MAPK (T202/Y204), phospho-S6 (S235/236), phospho-Akt (S473), Cleaved caspase 3, cleaved PARP, (Cell Signaling), tuberin, c-Myc (Santa Cruz), smooth muscle actin (BioGenex), beta-actin (Sigma), and Alexa Fluor® 488 Goat Anti-Rabbit IgG (H+L) antibody (Invitrogen).

Metabolomic profiling. 100 µg of frozen biopsy tissue was submitted to Metabolon, Inc. (Durham, NC) for sample extraction and analysis. In brief, Metabolon performed cold methanol extraction of mechanically disaggregated tissue samples and these extracts were split into three aliquots. The reproducibility of the extraction protocol was assessed by the recovery of xenobiotic compounds spiked into every tissue sample prior to extraction. These aliquots were processed and characterized by one of the three analytical methods previously described: UHPLC-ESI-MS/MS in the positive ion mode, UHPLC-ESI-MS/MS in the negative ion mode

and sialylation followed by GC-EI-MS. Chromatographic timelines were standardized using a series of xenobiotics that elute at specified intervals throughout each chromatographic run. The technical variability of each analytical platform was assessed by repeated characterization of a pooled standard that contained an aliquot of each sample within the study. Metabolon's global screening platform utilizes a non-targeted approach (Evans et al., 2009). For LC-MS/MS, after peak identification and quality control filtering (signal greater than 3x background, retention index within a pre-specified platform-dependent window, quant ions to library match within 0.4 m/z, and the MS/MS forward and reverse scores), the metabolites' relative concentrations were obtained from median-scaled day-block normalized data for each compound. In vitro data was normalized to total protein levels as measured by Bradford assay. Eicosanoids identified by the Metabolon platform in this study were measured by LC-MS/MS run in the negative mode. Fragmentation of the molecule's quant ion generated a pattern of ions that matched in mass and relative intensities to a purified standard as described by DeHaven et al. (Dehaven et al., 2010). In this study, the data were derived using a non-targeted method that does not incorporate labeled standards. However, in cases where targeted methods have been created and used to validate Metabolon screening platform, the results from the screening platform have shown a high degree of correlation with the targeted/absolute quantification methods and clinical measurements, when available (Sreekumar et al., 2009; Zhang et al., 2011).

Cell viability assay. Cell viability was determined by MTT assay (Sigma).

shRNA downregulation. 293T packaging cells were transfected with Rictor shRNA, or non-Targeting shRNA vectors using Mirus Trans-IT TKO Transfection reagent (Mirus). $Tsc2^{-/-}p53^{-/-}$ MEFs were infected with lentivirus containing Rictor shRNA, or non-Targeting shRNA. Cells

were harvested 48 hr post transfection and then selected against puromycin. Stable clones were harvested for future experiments.

Immunohistochemistry. Sections were deparaffinized, incubated with primary antibodies and biotinylated secondary antibodies and counterstained with Gill's Hematoxylin.

Quantification of prostaglandin levels. Levels of PGEM (a stable metabolite of PGE_2), 6-keto-$PGF_{1\alpha}$ (a stable metabolite of prostacyclin), and creatinine were measured using enzyme immunoassay (ELISA) kits (Cayman Chemical). Levels of secreted prostaglandins were normalized to vehicle control and expressed as fold change. Urinary levels of prostaglandins were normalized to creatinine levels and expressed as ng/mL.

Statistical analyses. Statistical analyses were performed using Student's t-test when comparing two groups for *in vitro* and *in vivo* studies. Two-Way ANOVO test was performed in xenograft tumor-aspirin studies. Mann Whitney tests were used for prostaglandin quantification in clinical data.

Author disclosure

Acknowledgments

References

Astrinidis, A., L. Khare, T. Carsillo, T. Smolarek, K.S. Au, H. Northrup, and E.P. Henske. 2000. Mutational analysis of the tuberous sclerosis gene TSC2 in patients with pulmonary lymphangioleiomyomatosis. *Journal of medical genetics* 37:55-57.

Auricchio, N., I. Malinowska, R. Shaw, B.D. Manning, and D.J. Kwiatkowski. Therapeutic trial of metformin and bortezomib in a mouse model of tuberous sclerosis complex (TSC). *PLoS One* 7:e31900.

Claria, J., M.H. Lee, and C.N. Serhan. 1996. Aspirin-triggered lipoxins (15-epi-LX) are generated by the human lung adenocarcinoma cell line (A549)-neutrophil interactions and are potent inhibitors of cell proliferation. *Molecular medicine* 2:583-596.

Costello, L.C., T.E. Hartman, and J.H. Ryu. 2000. High frequency of pulmonary lymphangioleiomyomatosis in women with tuberous sclerosis complex. *Mayo Clin. Proc.* 75:591-594.

Crino, P.B., K.L. Nathanson, and E.P. Henske. 2006. The tuberous sclerosis complex. *The New England journal of medicine* 355:1345-1356.

Dabora, S.L., S. Jozwiak, D.N. Franz, P.S. Roberts, A. Nieto, J. Chung, Y.S. Choy, M.P. Reeve, E. Thiele, J.C. Egelhoff, J. Kasprzyk-Obara, D. Domanska-Pakiela, and D.J. Kwiatkowski. 2001. Mutational analysis in a cohort of 224 tuberous sclerosis patients indicates increased severity of TSC2, compared with TSC1, disease in multiple organs. *Am. J. Hum. Genet.* 68:64-80.

Duvel, K., J.L. Yecies, S. Menon, P. Raman, A.I. Lipovsky, A.L. Souza, E. Triantafellow, Q. Ma, R. Gorski, S. Cleaver, M.G. Vander Heiden, J.P. MacKeigan, P.M. Finan, C.B.

Clish, L.O. Murphy, and B.D. Manning. Activation of a metabolic gene regulatory network downstream of mTOR complex 1. *Mol Cell* 39:171-183.

Egan, K.M., J.A. Lawson, S. Fries, B. Koller, D.J. Rader, E.M. Smyth, and G.A. Fitzgerald. 2004. COX-2-derived prostacyclin confers atheroprotection on female mice. *Science* 306:1954-1957.

FitzGerald, G.A., and C. Patrono. 2001. The coxibs, selective inhibitors of cyclooxygenase-2. *The New England journal of medicine* 345:433-442.

Galamb, O., S. Spisak, F. Sipos, K. Toth, N. Solymosi, B. Wichmann, T. Krenacs, G. Valcz, Z. Tulassay, and B. Molnar. 2010. Reversal of gene expression changes in the colorectal normal-adenoma pathway by NS398 selective COX2 inhibitor. *British journal of cancer* 102:765-773.

Henske, E.P., and F.X. McCormack. Lymphangioleiomyomatosis - a wolf in sheep's clothing. *J Clin Invest* 122:3807-3816.

Howe, S.R., M.M. Gottardis, J.I. Everitt, T.L. Goldsworthy, D.C. Wolf, and C. Walker. 1995a. Rodent model of reproductive tract leiomyomata. Establishment and characterization of tumor-derived cell lines. *Am. J. Pathol.* 146:1568-1579.

Howe, S.R., M.M. Gottardis, J.I. Everitt, and C. Walker. 1995b. Estrogen stimulation and tamoxifen inhibition of leiomyoma cell growth in vitro and in vivo. *Endocrinology* 136:4996-5003.

Jaeschke, A., J. Hartkamp, M. Saitoh, W. Roworth, T. Nobukuni, A. Hodges, J. Sampson, G. Thomas, and R. Lamb. 2002. Tuberous sclerosis complex tumor suppressor-mediated S6 kinase inhibition by phosphatidylinositide-3-OH kinase is mTOR independent. *J. Cell Biol.* 159:217-224.

Karbowniczek, M., A. Astrinidis, B.R. Balsara, J.R. Testa, J.H. Lium, T.V. Colby, F.X. McCormack, and E.P. Henske. 2003. Recurrent lymphangiomyomatosis after transplantation: genetic analyses reveal a metastatic mechanism. *American journal of respiratory and critical care medicine* 167:976-982.

Krymskaya, V.P. Treatment option(s) for pulmonary lymphangioleiomyomatosis: progress and current challenges. *Am J Respir Cell Mol Biol* 46:563-565.

Lee, P.S., S.W. Tsang, M.A. Moses, Z. Trayes-Gibson, L.L. Hsiao, R. Jensen, R. Squillace, and D.J. Kwiatkowski. 2010. Rapamycin-insensitive up-regulation of MMP2 and other genes in tuberous sclerosis complex 2-deficient lymphangioleiomyomatosis-like cells. *American journal of respiratory cell and molecular biology* 42:227-234.

Liu, F., E.P. Lunsford, J. Tong, Y. Ashitate, S.L. Gibbs, J. Yu, H.S. Choi, E.P. Henske, and J.V. Frangioni. Real-time monitoring of tumorigenesis, dissemination, & drug response in a preclinical model of lymphangioleiomyomatosis/tuberous sclerosis complex. *PLoS One* 7:e38589.

Manning. 2010. The Role of Target of Rapamycin Signaling in Tuberous Sclerosis Complex. In Tuberous Sclerosis Complex. V.H.W. D.J. Kwiatkowski, and E.A. Thiele, editor Wiley-VCH, Weinheim, Germany. 87-115.

McCormack, F.X., Y. Inoue, J. Moss, L.G. Singer, C. Strange, K. Nakata, A.F. Barker, J.T. Chapman, M.L. Brantly, J.M. Stocks, K.K. Brown, J.P. Lynch, 3rd, H.J. Goldberg, L.R. Young, B.W. Kinder, G.P. Downey, E.J. Sullivan, T.V. Colby, R.T. McKay, M.M. Cohen, L. Korbee, A.M. Taveira-DaSilva, H.S. Lee, J.P. Krischer, B.C. Trapnell, C. National Institutes of Health Rare Lung Diseases, and M.T. Group. 2011. Efficacy and

safety of sirolimus in lymphangioleiomyomatosis. *The New England journal of medicine* 364:1595-1606.

McCormack, F.X., Y. Inoue, J. Moss, L.G. Singer, C. Strange, K. Nakata, A.F. Barker, J.T. Chapman, M.L. Brantly, J.M. Stocks, K.K. Brown, J.P. Lynch, H.J. Goldberg, L.R. Young, B.W. Kinder, G.P. Downey, E.J. Sullivan, T.V. Colby, R.T. McKay, M.M. Cohen, L. Korbee, A.M. Taveira-Dasilva, H.S. Lee, J.P. Krischer, and B.C. Trapnell. Efficacy and Safety of Sirolimus in Lymphangioleiomyomatosis. *N Engl J Med*

McCormack, F.X., R.J. Panos, and B.C. Trapnell, editors. 2010. Molecular Basis of Pulmoanry Disease

Insights from Rare Lung Disorders. Human Press, New York.

McCormack, F.X., W.D. Travis, T.V. Colby, E.P. Henske, and J. Moss. Lymphangioleiomyomatosis: calling it what it is: a low-grade, destructive, metastasizing neoplasm. *Am J Respir Crit Care Med* 186:1210-1212.

Muller, R. 2004. Crosstalk of oncogenic and prostanoid signaling pathways. *Journal of cancer research and clinical oncology* 130:429-444.

Neuman, N.A., and E.P. Henske. Non-canonical functions of the tuberous sclerosis complex-Rheb signalling axis. *EMBO Mol Med* 3:189-200.

Onda, H., A. Lueck, P.W. Marks, H.B. Warren, and D.J. Kwiatkowski. 1999. Tsc2(+/-) mice develop tumors in multiple sites that express gelsolin and are influenced by genetic background. *The Journal of clinical investigation* 104:687-695.

Parkhitko, A., F. Myachina, T.A. Morrison, K.M. Hindi, N. Auricchio, M. Karbowniczek, J.J. Wu, T. Finkel, D.J. Kwiatkowski, J.J. Yu, and E.P. Henske. Tumorigenesis in tuberous sclerosis complex is autophagy and p62/sequestosome 1 (SQSTM1)-dependent. *Proc Natl Acad Sci U S A*

Plank, T.L., R.S. Yeung, and E.P. Henske. 1998. Hamartin, the product of the tuberous sclerosis 1 (TSC1) gene, interacts with tuberin and appears to be localized to cytoplasmic vesicles. *Cancer Res.* 58:4766-4770.

Ryu, J.H., T.E. Hartman, V.E. Torres, and P.A. Decker. 2012. Frequency of undiagnosed cystic lung disease in patients with sporadic renal angiomyolipomas. *Chest* 141:163-168.

Sevigny, M.B., C.F. Li, M. Alas, and M. Hughes-Fulford. 2006. Glycosylation regulates turnover of cyclooxygenase-2. *FEBS letters* 580:6533-6536.

Strizheva, G.D., T. Carsillo, W.D. Kruger, E.J. Sullivan, J.H. Ryu, and E.P. Henske. 2001. The spectrum of mutations in TSC1 and TSC2 in women with tuberous sclerosis and lymphangiomyomatosis. *American journal of respiratory and critical care medicine* 163:253-258.

Subbaramaiah, K., P.G. Morris, X.K. Zhou, M. Morrow, B. Du, D. Giri, L. Kopelovich, C.A. Hudis, and A.J. Dannenberg. Increased levels of COX-2 and prostaglandin E2 contribute to elevated aromatase expression in inflamed breast tissue of obese women. *Cancer Discov* 2:356-365.

Takada, Y., A. Bhardwaj, P. Potdar, and B.B. Aggarwal. 2004. Nonsteroidal anti-inflammatory agents differ in their ability to suppress NF-kappaB activation, inhibition of expression of cyclooxygenase-2 and cyclin D1, and abrogation of tumor cell proliferation. *Oncogene* 23:9247-9258.

Taveira-Dasilva, A.M., G. Pacheco-Rodriguez, and J. Moss. The natural history of lymphangioleiomyomatosis: markers of severity, rate of progression and prognosis. *Lymphat Res Biol* 8:9-19.

Wang, D., and R.N. Dubois. Eicosanoids and cancer. *Nat Rev Cancer* 10:181-193.

Wang, M.T., K.V. Honn, and D. Nie. 2007. Cyclooxygenases, prostanoids, and tumor progression. *Cancer metastasis reviews* 26:525-534.

Yu, J., A. Astrinidis, S. Howard, and E.P. Henske. 2004. Estradiol and tamoxifen stimulate LAM-associated angiomyolipoma cell growth and activate both genomic and nongenomic signaling pathways. *American journal of physiology. Lung cellular and molecular physiology* 286:L694-700.

Yu, J., and E.P. Henske. 2010. Dysregulation of TOR Signaling in Tuberous Sclerosis and Lymphangioleiomyomatosis. In The Enzyme. Academic Press, Burlington. 303-327.

Yu, J.J., V.A. Robb, T.A. Morrison, E.A. Ariazi, M. Karbowniczek, A. Astrinidis, C. Wang, L. Hernandez-Cuebas, L.F. Seeholzer, E. Nicolas, H. Hensley, V.C. Jordan, C.L. Walker, and E.P. Henske. 2009. Estrogen promotes the survival and pulmonary metastasis of tuberin-null cells. *Proceedings of the National Academy of Sciences of the United States of America* 106:2635-2640.

Figure Legends

Figure 1. Identification of an estradiol-induced prostaglandin biosynthesis signature in TSC2-deficient cells and preclinical models. (**a**) ELT3 (Tsc2-deficient rat uterus-derived) cells were treated with 10 nM estradiol for 24 hr. Cellular metabolites were profiled by mass spectrometry (n = 5) (Metabolon LC-MS/MS). Box-plots of PGE_2 (6.0 ng - 59.6 ng), PGD_2 (1.3 ng - 7.2 ng), and 6-keto $PGF_{1\alpha}$ (2.5 ng - 18.3 ng) are shown. Data show the mean of five sets of independent samples. (**b**) Immunoblot analysis of ELT3 cells treated with estradiol for 2 or 24 hr. Beta-actin was used as a loading control. (**c, d**) Secreted PGE_2 levels were measured in conditioned media collected from cells treated with estradiol or control at the indicated times, data were normalized to control group (n = 3) (ELISA). Results are representative of six sets of independent samples per group from three experiments. (**e, f**) LAM patient-derived cells were serum-starved for 24 hr, and then treated with estradiol for 0.25, 0.5, 2, 4, 6, 8, or 24 hr. Immunoblot analyses of tuberin, phospho-Akt S473, phospho-MAPK (T202/Y204), and phospho-S6 (S235/236). (**g, h**) Immunoblot analyses of COX-2, phospho-S6 (S235/236), phospho-MAPK (T202/Y204) and phospho-Akt S473. (**i, j**) LAM patient-derived cells treated with 50 μM PD98059, or 5 μM PI-103 for 1 hr, and then treated with 10 nM estradiol for 24 hr. Immunoblot analyses of COX-2, phospho-S6 (S235/236), phospho-MAPK (T202/Y204) and phospho-Akt S473. (e-j) Results are representative of three different experiments. (**k**) Levels of phospho-MAPK (Thr202/Tyr204) and phospho-S6 (Ser235/236) from xenograft tumors from placebo or estradiol-treated CB17-scid mice were measured by immunoblotting. (**l**) Cellular metabolites extracted from xenograft tumors from estradiol or placebo-treated mice were profiled (n = 8) (Metabolon LC-MS/MS). Box-plots of PGE_2 (23.3 ng - 133 ng), PGD_2 (6.8 ng - 76.96 ng), and 6-keto $PGF_{1\alpha}$ (17.5 ng - 167.3 ng) are shown. (k, l) Results are representative of

25

eight mice per group. (**m**) Urinary PGE$_2$ and creatinine from placebo or estradiol-implanted ovariectomized female mice bearing xenograft tumors was measured five-week post cell inoculation (ELISA). PGE$_2$ levels were normalized to creatinine. Results are representative of four mice per group. * $p < 0.05$, ** $p < 0.01$.

Figure 2. TSC2 negatively regulates COX-2 expression and prostaglandin production in a rapamycin-insensitive but Torin 1 and mTORC2-dependent manner *in vitro*. (**a**) Simplified prostaglandin biosynthesis pathway. (**b**) Re-analysis of previously published expression array data (Lee et al, 2009). Bar graph of the transcript levels of *PTGS2* (COX-2) and *PTGIS* (prostacyclin synthase) in TSC2-deficent (TSC2-) and TSCS2-addback (TSC2+) LAM patient-derived cells treated with rapamycin (Rapa) or Vehicle for 24 hr. Data show the mean of three sets of independent samples. (**c**) Real-time RT-PCR analysis of the transcript levels of *PTGS2* and *PTGIS* in TSC2-deficient LAM patient-derived cells relative to TSC2-addback cells treated with 20 nM rapamycin or vehicle for 24 hr. Data show the mean of three sets of independent samples. (**d,e,f**) Immunoblot analyses of tuberin, PTGIS, phospho-S6 (S235/236) and COX-2 protein in LAM patient-derived cell treated with 20 nM rapamycin (Rapa), 1 μg/mL tunicamycin (TN), or rapamycin plus tunicamycin, for 24 hr. Results are representative of three different experiments. (**e, g**) Secreted prostaglandin levels were quantified in conditioned media collected from LAM patient-derived cells treated with 20 nM rapamycin (Rapa), 1 micro g/mL tunicamycin (TN), or rapamycin plus tunicamycin, for 24 hr (n = 3) (ELISA). Results are representative of three sets of independent samples per group. (**h**) ELT3 cells were treated with 20 nM rapamycin (Rapa) or control for 24 hr. Immunoblot analysis of COX-2 and phospho-S6 (S235/236). Results are representative of three different experiments. (**i**) Secreted prostaglandin levels were quantified in conditioned media collected from ELT3 cells treated with rapamycin or

control, data were normalized to control group (n = 3) (ELISA). Results are representative of three sets of independent samples per group. (**j**) HeLa, OVCAR-5 and U2OS cells were treated with 20 nM rapamycin for 24 hr. Immunoblot analysis of COX-2 and phospho-S6 (S235/236). Results are representative of three different experiments. (**k**) Secreted prostaglandin levels were quantified in conditioned media collected from cells treated with rapamycin or control, data were normalized to control group (n = 3) (ELISA). Results are representative of three sets of independent samples per group. * $p < 0.05$, ** $p < 0.01$, *** $p < 0.005$, **** $p < 0.001$.

Figure 3. TSC2 negatively regulates COX-2 expression and prostaglandin production in a xenograft tumor model of ELT3 cells. Female CB17-scid mice were inoculated with ELT3-V3 cells (TSC2-, vector addback) or TSC2 addback (TSC2+) ELT3-T3 cells subcutaneously. (**a, d**) Immunoblot analysis shows levels of <u>phospho-S6 (S235/236), COX-2 and PTGIS</u> in xenograft tumors of ELT3 cells. (**b**) Levels of PGE_2 in xenograft tumors and (**c**) Urinary levels of PGE_2 and (**e**) 6-keto-$PGF_{1\alpha}$ were normalized to creatinine levels in mice bearing xenograft tumors (n = 9) (ELISA). Results are representative of five to nine mice per group. *** $p < 0.001$.

Figure 4. mTORC2 regulates COX-2 expression via PI3K/AKT pathway in TSC2-deficient cells. (**a**) *Tsc2$^{-/-}$p53$^{-/-}$* MEFs were treated with 20 nM rapamycin, 250 nM Torin 1, or 20 μM LY294002 for 24 hr. Levels of COX-2, 4EBP1, phospho-S6 (S235/236) were assessed by immunoblot. (**b & c**) *Tsc2$^{-/-}$p53$^{-/-}$* MEFs were transfected with Rictor shRNA or control shRNA, and then selected with puromycin to obtain stable cells. Control shRNA or with Rictor shRNA-*Tsc2$^{-/-}$p53$^{-/-}$* MEFs were treated with vehicle or 20 nM rapamycin for 24 hr. Levels of COX-2, COX-1, phospho-S6 (S235/236), and phospho-Akt (S473) were assessed by immunoblot. (**d**) LAM patient-derived cells (TSC2-) cells were treated with 20 nM rapamycin, or 250 nM Torin 1, or 50 μM NS398 for 24 hr. Levels of COX-2 and phospho-S6 (S235/236) were assessed by

immunoblot. (**e**) TSC2-deficient LAM patient-derived cells were treated with 250 nM Torin 1 for 24 hr. Levels of COX-2, phospho-p44/42-MAPK, phospho-Akt S473, phospho-S6 (S235/236) were assessed by immunoblot. (**f**) TSC2-deficient LAM patient-derived cells were treated with 5 μM PI-103 or 5 μM AKTVIII for 24 hr. Levels of COX-2 and phospho-Akt (S473) were assessed by immunoblot. (**g**) TSC2-deficient LAM patient-derived cells were treated with 50 μM PD98059, 5 μM PI-103, or PD98059 plus PI-103 for 24 hr. Levels of COX-2, phospho-Akt S473, phospho-p44/42-MAPK, and phospho-S6 (S235/236) were assessed by immunoblot. (**h**) TSC2-deficient LAM patient-derived cells were treated with 1 μM Gefitinib, or 1 μM Afatinib for 24 hr. Levels of COX-2, EGFR, and phospho-Akt S473 were assessed by immunoblot. (**i**) ELT3 cells expressing empty vector (TSC2-) and TSC2-addback (TSC2+), or LAM patient-derived cells (TSC2-) cells and TSC2-addback cells (TSC2+) were treated with 20 nM rapamycin (Rapa) for 24 hr. Subcellular localization of EGFR was examined using confocal microscopy. (**j**) Cells were treated with 50 μM Sulindac, 50 μM NS398, or 450 μM aspirin for 24 hr. Levels of COX-1, COX-2, phospho-p44/42 MAPK and phospho-S6 were assessed by immunoblot. (a-j) Results are representative of two to four different experiments. (**k**) PGE$_2$ levels from conditioned media were measured (ELISA). Results are representative of six sets of independent samples per group. (**l**) Cell proliferation after drug treatment was measured using MTT assay. Results are representative of twelve sets of independent samples per group. * p < 0.05.

Figure 5. Inhibition of COX-2 suppresses renal tumorigenesis and inhibits the progression of xenograft tumor of Tsc2-deficient cells in preclinical models. (**a & b**) *Tsc2*$^{+/-}$ mice were treated with either vehicle or Celecoxib (0.1% in mouse chow) for one month, and then sacrificed for analysis at the end of treatment. Renal cystadenoma histology and microscopic

kidney tumor scores were assessed. (**a**) Microscopic kidney tumor scores are plotted on a linear scale (p=0.0002). Data are analyzed from 16 Vehicle and 11 Celecoxib treatment groups. (**b**) Two cystadenomas each are shown at 10x, with a portion of the tumor shown at 20x. Results are representatives of 11 or 16 mice per group. (**c-g**) Female CB17-scid mice were inoculated with ELT3-luciferase cells subcutaneously. Mice were treated with either vehicle or aspirin (100 mg/kg/day in the drinking water) for three weeks (n=9). Results are representative of five to eight mice per group. (**c, d**) Bioluminescent imaging was performed weekly. Bioluminescent intensity in xenograft tumors was recorded and quantified weekly. Data are the mean of bioluminescent intensityin tumors from five to eight mice per group. (**e**) Tumor area was normalized to the baseline before drug administration. Data represent the mean of tumor area from five to eight mice per group. (**f**) Immunoblot analysis of COX-2, c-Myc, and phospho-S6 in xenograft tumors from mice treated with aspirin or vehicle. Results represent tumors from five mice from each group. (**g**) Mouse urinary levels of PGE_2 were measured (ELISA). Data represent the mean of PGE_2 levels from five to eight mice per group. * $p < 0.05$, ** $p < 0.01$, *** $p < 0.001$.

Figure 6. COX-2 expression and prostaglandin production in LAM nodules and LAM patients. (**a**) Transcript levels of *PTGS2* (COX-2), were measured using real-time RT-PCR on RNA prepared from LAM lung and clinically normal lung samples (n = 3 each). Data represent the mean of PTGS2 levels from three subjects from per group. (**b**) LAM lung tissues stained with COX-2 antibody. Scale bar, 62.5 µm or 250 µM. Results are representative of six cases. (**c**) Exhaled breath condensates (EBCs) were collected from LAM patients before and after aspirin (ASA) treatment (81 mg/day) for two weeks. Levels of 15-epi-LXA$_4$ were quantified (n = 3). Data represent the mean of 15-epi-LXA4 levels from three subjects from per group. (**d**) 621-101

cells were incubated with 100 nM 15-epi-LXA$_4$ for 0, 24, 48 and 72 hr. Cell proliferation was measured using MTT assay. Results are representative of one out of three experiments including twelve sets of samples in each experiment. (**e**) The 15-epi-LXA4 integrity was confirmed by UV-Vis spectrophotometry to ensure the presence of the diagnostic tetraene chromophore and accurate quantitation and HPLC to ensure that only a single peak was present without evidence for isomerization. 621-101 cells were incubated with 10, 20, 100, 200 or 500 nM 15-epi-LXA$_4$ for 72 hr. Cell proliferation was measured using MTT assay. Results are representative of one out of two experiments including 16 sample sets in each experiment. (**f**) Urine samples were collected from LAM patients and healthy women from two geographic locations. Urinary levels of PGE$_2$ in LAM (n = 29) and healthy women (N) (n = 18) were assessed (ELISA). Serum levels of PGE$_2$ (**g**) and 6-keto PGF$_{1\alpha}$ (**h**) in LAM (n = 14) and healthy women (N) (n = 13) were assessed (ELISA). * $p < 0.05$, ** $p < 0.01$.
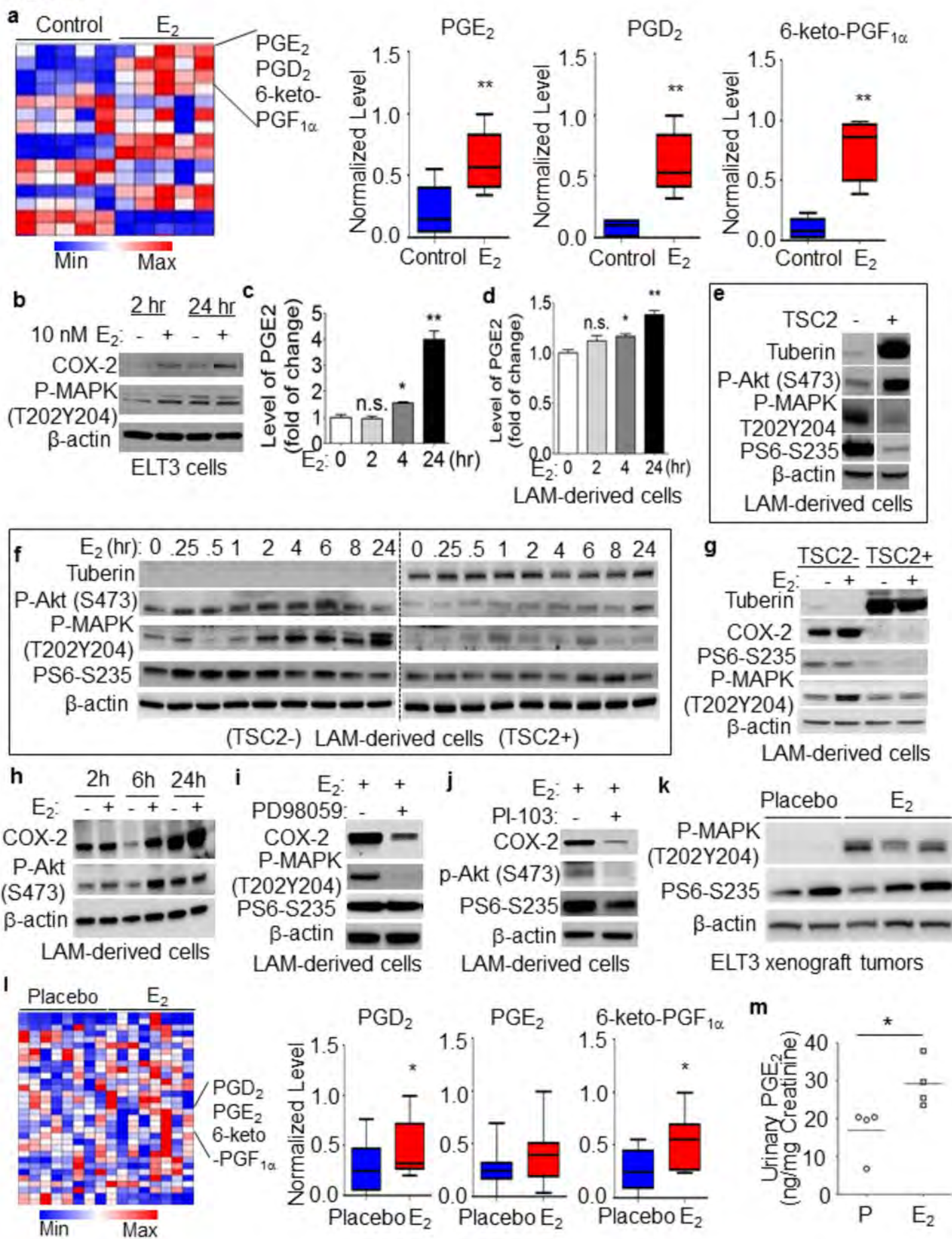
Tables

Table 1. Rapamycin-insensitive upregulation of *PTGS2* and *PTGIS* expression in TSC2-deficient LAM patient-derived cells compared to TSC2 reexpressing cells, are not affected by rapamycin treatment.

Gene	Protein	Fold change TSC2-/vehicle vs TSC2+/vehicle	Fold change TSC2-rapamycin vs TSC2-/vehicle	Fold change TSC2-/rapamycin vs TSC2+/vehicle
PTGS2	Cyclooxygenase-2 (COX-2)	2.1 ($p = 0.004$)	1.3 ($p = 0.05$)	2.8 ($p = 0.0006$)
PTGIS	Prostacyclin synthase (PGIS)	40.4 ($p = 0.00001$)	1.5 ($p = 0.0006$)	61.1 ($p = 0.000003$)

Table 2. Clinical profile of LAM subjects.

	Subject 1	Subject 2	Subject 3
Age	34	47	38
Type of LAM	Sporadic	TSC	Sporadic
Date of Diagnosis	Nov-06	Feb-03	Jan-05
FEV1 (%)	104	70	108
Pneumothorax	No	Yes	No
Pleurodesis procedure	No	Yes	No
Pleural effusion/chylothotax	No	No	No
Hemoptysis	No	No	No

Figure 1
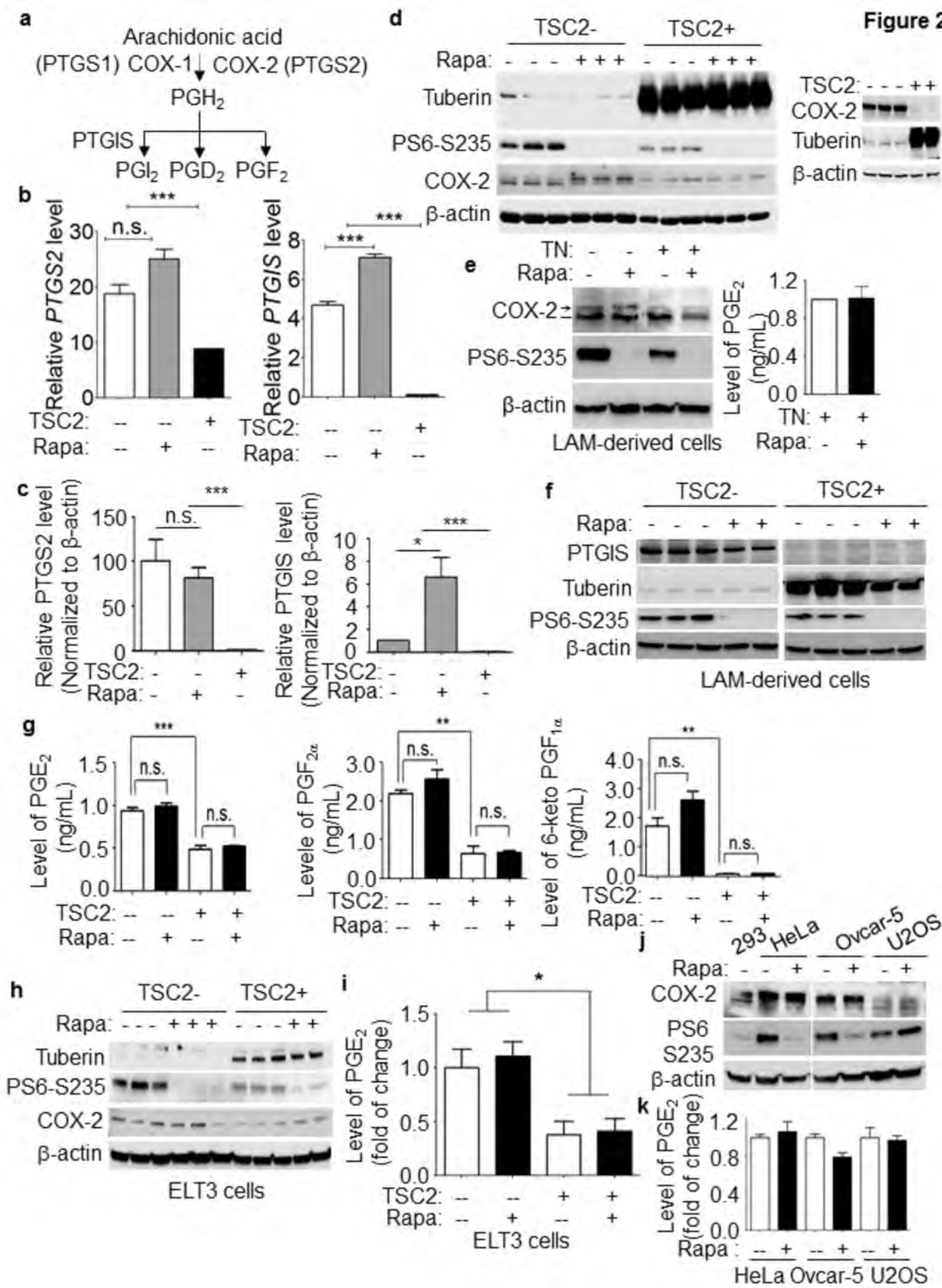
Figure 2

Figure 3

Figure 4

Figure 5

a

Tumor volume per kidney (mm³)

***

Vehicle (n = 32)   Celecoxib (n = 22)

b

| H&E (10x) | H&E (20x) | H&E (10x) | H&E (20x) |

Veh

Celecoxib

Kidney of $Tsc2^{+/-}$ mice

c

Bioluminescent images

Vehicle   Aspirin

W0
W1
W2
W3

d

Bioluminescent intensity (fold change)

□ Vehicle   ■ Aspirin

**

0   1   2   3 (wk)

e

Tumor Area (Fold change)

□ Vehicle   ■ Aspirin

*

0   1   2   3 (wk)

f

Aspirin − − − − − + + + + +

COX-2
β-actin

c-MYC
PS6-S235
Cl-Caspase-3 (Asp175)
Cl-PARP (Asp214)
β-actin

g

Urinary PGE₂ (ng/mg Creatinine)

□ Vehicle   ■ Aspirin

*   ***

Baseline   0   1   2   3 (wk)

Figure 6

a Transcript levels (PTGS2 to β-actin)
NL   LAM
*

b
62.5 μm
62.5 μm
62.5 μm
62.5 μm

c 15-epi-LXA$_4$ (pg/EBC)
Before   After
Aspirin treatment

d 15-epi-LXA$_4$ temporal response
Cell growth (fold change)
□ Vehicle
■ 15-epi-LXA$_4$ (100 nM)
0   24   48   72 (hr)
*
**

e Absorbance (AU)
15-epi-LXA$_4$
260   300   340   380
Wavelength (nm)
301nm   15-epi-LXA4
(mAU)
5   10   15   20

15-epi-LXA$_4$ dose response (72 hr)
Cell growth (fold change)
0   10   20   100   200   500 (nM)
**   ***   ***

f Urinary PGE$_2$ (ng/mg Creatinine)
N   LAM
n.s.

g Serum PGE$_2$ (pg/mL)
N   LAM
**

h Serum 6-keto-PGF$_{1α}$ (pg/mL)
N   LAM
**